Environmental Advances 8 (2022) 100235

Contents lists available at ScienceDirect

Environmental Advances

journal homepage: www.sciencedirect.com/journal/environmental-advances

A triple threat: Ocean warming, acidification, and rare earth elements exposure triggers a superior antioxidant response and pigment production in the adaptable *Ulva rigida*

Cátia Figueiredo [a,b,c,*], Tiago F. Grilo [a], Rui Oliveira [b], Inês João Ferreira [d], Fátima Gil [e], Clara Lopes [b,f], Pedro Brito [b,f], Pedro Ré [a], Miguel Caetano [b,f], Mário Diniz [c,g], Joana Raimundo [b,f]

[a] MARE – Marine and Environmental Sciences Centre, Faculdade de Ciências da Universidade de Lisboa, Campo Grande, Lisboa 1749-016, Portugal
[b] Division of Oceanography and Marine Environment, IPMA – Portuguese Institute for Sea and Atmosphere, Av. Alfredo Magalhães Ramalho, 6, Algés 1495-165, Portugal
[c] Associate Laboratory i4HB - Institute for Health and Bioeconomy, School of Science and Technology, NOVA University Lisbon, Caparica 2819-516, Portugal
[d] LAQV-REQUIMTE, Chemistry Department, NOVA School of Science and Technology, Caparica 2829-516, Portugal
[e] Aquário Vasco da Gama, Rua Direita do Dafundo, Cruz Quebrada 1495-718, Portugal
[f] CIIMAR – Interdisciplinary Centre of Marine and Environmental Research, Avenida General Norton de Matos S/N, 4450-208 Matosinhos, Portugal
[g] UCIBIO – Applied Molecular Biosciences Unit, Department of Chemistry / Department of Life Sciences, School of Science and Technology, NOVA University Lisbon, Caparica 2819-516, Portugal

ARTICLE INFO

Keywords:
Green macroalgae
Lanthanum
Gadolinium
Oxidative stress
Total chlorophyll
Carotenoid content

ABSTRACT

Anthropogenic increased atmospheric CO_2 concentrations will lead to a drop of 0.4 units of seawater pH and ocean warming up to 4.8°C by 2100. Contaminant's toxicity is known to increase under a climate change scenario. Rare earth elements (REE) are emerging contaminants, that until now have no regulation regarding maximum concentration and discharge into the environment and have become vital to new technologies such as electric and hybrid-electric vehicle batteries, wind turbine generators and low-energy lighting. Studies of REE, namely Lanthanum (La) and Gadolinium (Gd), bioaccumulation, elimination, and toxicity in a multi-stressor environment (e.g., warming and acidification) are lacking. Hence, we investigated the algae phytoremediation capacity, the ecotoxicological responses and total chlorophyll and carotenoid contents in *Ulva rigida* during 7 days of co-exposure to La or Gd (15 μg L^{-1} or 10 μg L^{-1}, respectively), and warming and acidification. Additionally, we assessed these metals elimination, after a 7-day phase. After one day of experiment La and Gd clearly showed accumulation/adsorption in different patterns, at future conditions. Unlikely for Gd, Warming and Acidification contributed to the lowest La accumulation, and increased elimination. Lanthanum and Gd triggered an adequate activation of the antioxidant defence system, by avoiding lipid damage. Nevertheless, REE exposure in a near-future scenario triggered an overproduction of ROS that requested an enhanced antioxidant response. Additionally, an increase in total chlorophyll and carotenoids could also indicate an unforeseen energy expense, as a response to a multi-stressor environment.

1. Introduction

Since the industrial revolution that exacerbated anthropogenic CO_2 emissions are striking physicochemical changes in seawater. The Intergovernmental Panel on Climate Change (IPCC) projects that these abnormal atmospheric CO_2 concentrations will lead to a drop of up to 0.4 units of seawater pH, by the end of the 21st century, in a worst-case scenario, in the Mediterranean Sea and North Atlantic Ocean (i.e., SSP5-8.5; IPCC, 2021). Besides this known ocean acidification phenomenon, increasing atmospheric CO_2 levels will also allude, among others, to global average temperature increase, with direct implications in seawater temperature. The IPCC predicts warming of the mean sea surface temperature between 3.3 and 3.9°C for the same timeframe, in the North Atlantic Ocean and Mediterranean Sea (IPCC, 2021).

* Corresponding author at: MARE – Marine and Environmental Sciences Centre, Faculdade de Ciências da Universidade de Lisboa, Campo Grande, Lisboa 1749-016, Portugal.
E-mail address: cafigueiredo@fc.ul.pt (C. Figueiredo).

https://doi.org/10.1016/j.envadv.2022.100235
Received 23 March 2022; Received in revised form 20 April 2022; Accepted 4 May 2022
Available online 13 May 2022

The enhancement of contaminants toxicity is also known to be caused by climate change (Figueiredo et al., 2020). The increase in seawater temperature can affect the bioavailability of pollutants, through transport and change in speciation, while altering the metabolism of the biota, its physiology and aptitude, affecting the patterns of bioaccumulation and elimination of contaminants (Maulvault et al., 2016).

Emerging contaminants constitute another difficulty, particularly to coastal environments and their inhabitants. Rare earth elements (REE) belong to this category of contaminants (i.e., emergent), and have become in recent years of chief importance to the manufacture of new technologies, such as electric and hybrid-electric vehicle batteries, wind turbine generators and low-energy lighting (Atwood, 2013). The REE are a family of 17 elements, composed of the 15 lanthanides, plus yttrium, and scandium. In the present study, Lanthanum (La) and Gadolinium (Gd) were chosen as representatives of Light (LREE) and Heavy REE (HREE), respectively. These chemical elements are applied in medicine as magnetic resonance imaging contrast, agriculture, animal husbandry, and aquaculture (Gwenzi et al., 2018). Additionally, the growing demand for modern electronic products has led to an alarming build-up of electronic waste (e-waste). E-waste dismantling, storage, and burning can release its components into the environment (Uchida et al., 2018). Furthermore, the recycling of REE is until recently rarely applied due to inefficient techniques (Binnemans et al., 2021). Increased REE usage, in the recent past, has resulted in increased discharge into the environment and the transfer to aquatic ecosystems is expected to be upheld. Natural concentrations of REE in river water may reach up to 200 ng L^{-1}, while La and Gd levels near wastewater outfalls may reach up to 0.08 and 1.1 mg L^{-1}, respectively (Migaszewski et al., 2015; Trapasso et al., 2021). While Elderfield et al. (1990) described natural REE levels in seawater up to 40 ng L^{-1}, the increasing usage and consequent discharge into the environment may further disrupt the natural REE pattern in seawater bodies in the near future. The risks associated with excess REE availability in the aquatic environment have gathered the scientific community's attention in recent years, however still little and quite puzzling information is available on its uptake and toxicity. Furthermore, integrated studies dealing with REE bioaccumulation and toxicity in a multi-stressor environment (e.g., warming and acidification) are lacking.

Another human created problematic is the increased urbanization and coastal zone use that leads to coastal eutrophication (Smith et al., 1999). This together with changing climatic conditions promotes green tide events. *Ulva* sp. (Chlorophyta) are generally the dominant genus of green tides (reviewed in Fletcher, 1996). This genus is common worldwide and is dominant along marine coasts (Uchimura et al., 2004). Macroalgae can accumulate a wide array of metals, and this has led to their appliance as biomonitors of water contamination. Particularly, *Ulva* spp. present a strong capacity to trap emerging pollutants such as REE (e.g., Pinto et al., 2020) and microplastics (Feng et al., 2020, 2021). Nevertheless, to the best of our knowledge, a study of the interactive effects of ocean warming, acidification, and REE with an algae species has never been conducted. In this context, we investigated the potential for phytoremediation, the ecotoxicological responses (antioxidant enzymes and cellular oxidative damage) and total chlorophyll and carotenoid contents in *U. rigida* after 7 days of co-exposure to La or Gd (15 μg L^{-1} or 10 μg L^{-1}, respectively), and warming and acidification. Furthermore, we assessed the bioaccumulation and elimination of La or Gd, after a seven-day exposure and seven-day elimination period.

2. Material and methods

2.1. Specimens acquisition

Fresh *U. rigida* thalli were collected manually in a single sampling event in April 2021 at a land-based aquaculture system (ALGAplus Ltda). This company produces macroalgae at Ria de Aveiro lagoon (40º 36′ 44.7″ N, 8º 40′ 27.0″ W) in coastal Portugal under the EU organic aquaculture standards (EC710/ 2009). *Ulva rigida* was immediately transported in aerated and controlled temperature seawater from its source of origin, under refrigerated conditions (+4°C), until reaching the aquaculture facilities of Aquário Vasco da Gama, in Lisbon. Before acclimation, the seaweed blades were rinsed with filtered seawater to remove epiphytes and debris. Roughly eight thousand and two hundred thalli disks of 15 mm in diameter were cut to warrant homogeneity in weight and exposure area and placed in gently aerated filtered seawater in a 12 h:12 h light-dark cycle (irradiance of 45 μmol photons m^{-2} s^{-1}, fluorescent tubes, Philips) and at the same physicochemical parameters as the sample location (T = 18°C, pH = 8.1, salinity = 35 PSU). The disks were acclimated for 5 days.

2.2. Experimental design

Seaweed disks were distributed in glass tanks representative of 12 experimental treatments: (i) Control temperature and pH (18°C, pH = 8.1, ~400 μatm pCO_2); (ii) Acidification (18°C, pH = 7.7, ~900 μatm pCO_2); (iii) La exposure (18°C, pH = 8.1, ~400 μatm pCO_2, added La = 15 μg L^{-1}); (iv) Acidification & La (18°C, pH = 7.7, ~900 μatm pCO_2, added La = 15 μg L^{-1}); (v) Gd exposure (18°C, pH = 8.1, ~400 μatm pCO_2, added Gd = 10 μg L^{-1}); (vi) Acidification & Gd (18°C, pH = 7.7, ~900 μatm pCO_2, added Gd = 10 μg L^{-1}); (vii) Warming (22°C, pH = 8.1, ~400 μatm pCO_2); (viii) Warming & acidification (22°C, pH = 7.7, ~900 μatm pCO_2); (ix) Warming & La (22°C, pH = 8.1, ~400 μatm pCO_2, added La = 15 μg L^{-1}); (x) Warming, acidification & La (22°C, pH = 7.7, ~900 μatm pCO_2, added La = 15 μg L^{-1}); (xi) Warming & Gd (22°C, pH = 8.1, ~400 μatm pCO_2, added Gd = 10 μg L^{-1}); (xii) Warming, acidification & Gd (22°C, pH = 7.7, ~900 μatm pCO_2, added Gd = 10 μg L^{-1}). The studied abiotic values were selected according to the SSP5-8.5 scenario for the year 2100 (IPCC, 2021), for the North Atlantic and the Mediterranean, as the sampling location is influenced by both water masses (Cunha, 2001). Natural seawater was pumped directly from the ocean, and subsequently filtered (0.35 μm filters) and UV-sterilized (Vecton600, TMC Iberia). Seawater temperature was adjusted by heaters (V2Therm, TMC Iberia) and chillers (HC-250A, Hailea) submerged in a water bath, together with the twelve experimental glass tanks. Seawater pH was automatically regulated through a Profilux system (3.1, GHL), coupled to pH probes (GHL). Solenoid valves connected to this system downregulated automatically the seawater pH through injecting CO_2 enriched air. Upregulation was done by injecting filtered air. The seawater temperature (thermometer TFX 430, WTW GmbH), pH (pH/ion meter SG8, Mettler-Toledo) and salinity (V2 Refractometer, TMC) were hand monitored daily. Seawater carbonate system speciation was calculated every sampling day from total alkalinity (Alkalinity checker, Hanna) and pH measurements, using the CO2SYS software.

As La and Gd is stable in seawater for at least 24 h (Figueiredo et al., 2022), during the exposure phase, a La or a Gd spike-solution ($LaCl_3$ and $GdCl_3$, Merck, respectively) was added to the renewed water every other day in the corresponding exposure treatments to assure the dissolved levels. The La and Gd exposure concentrations (15 μg L^{-1} or 10 μg L^{-1}, respectively) were selected having in consideration values reported in contaminated aquatic systems (Åström, 2001; González et al., 2015; Rogowska et al., 2018). Water aliquots were sampled after 24h of exposure in every experimental tank, filtered for particles removal (0.45 μm Millipore), and acidified (20% ultrapure HNO_3) to determine La and Gd levels.

Ulva rigida was sampled immediately before the beginning of the trial (T0), and after 1 (T1), 3 (T3), and 7 days (T7). Following, a 7-day elimination phase began (T14), where no La nor Gd solutions were added. During the entire experiment, the media was completely renewed every two days.

After being sampled, *U. rigida* was stored at -80°C until further analyses.

2.3. La and Gd quantification

Five pools of 30 *U. rigida* disks were used for La and Gd quantification. The pools were freeze-dried, grounded, and homogenized before being digested in a microwave CEM MArsXpress with nitric acid (HNO_3, distilled, 65% v/v) as in Brito et al. (2020). The labware used in this procedure was previously decontaminated with HNO_3 (20%).

Concentrations of La and Gd were determined in a quadrupole ICP-MS (NexION 2000C). ^{115}In was used as an internal standard (Alfa Aesar, Plasma Standard Solution, Specpure®, In 1000 μg mL^{-1}). The ^{139}La and ^{158}Gd were the quantified isotopes, as they present minimum isobaric and polyatomic interferences under routine conditions ($^{137}Ba^{++}/^{137}Ba$ and $^{140}Ce^{16}O/^{140}Ce \approx 0.010$). Three procedural blanks were included within each batch of 20 samples and accounted for less than 1% of the total concentrations determined in the samples. The accuracy of the analytic method was also evaluated through the evaluation of an international certified material (BCR 668). The results obtained did not differ significantly ($p > 0.05$) from the certified values and the percentage recovery was 90 ± 11%. The La and Gd ICP-MS detection limit for *U. rigida* samples were 0.12 and 0.032 μg L^{-1}, respectively.

Water samples were preconcentrated using an automated Elemental Scientific Inc. SeaFAST system (SeaFASTpico™) prior to analysis by ICP-MS (NexION 2000C) following the methodology described by Hatje et al. (2014). Succinctly, acidified seawater sampled were spiked with a standard containing known isotopic ratios. Like the algae samples, water samples were run with blanks, seawater quality controls and certified reference materials (CASS-6 and NASS-7). A six-point calibration curve was used, and the detection limit was determined through the method blanks. The La and Gd ICP-MS detection limit for seawater samples were 0.008 and 0.003 μg L^{-1}, respectively.

Accumulated concentrations are presented in microgram per gram of tissue dry weight (μg g^{-1}, dw) and La and Gd levels in water are presented in microgram per litre (μg L^{-1}).

2.4. Bioaccumulation and elimination factor

The La and Gd bioaccumulation factor and elimination coefficient were calculated as in Figueiredo et al. (2018) to assess *Ulva rigida*'s accumulation effectiveness and recover ability.

2.5. Biochemical analyses

A total of $n = 4$ disks for each of the 12 treatments were sampled for biochemical analyses, each sampling time.

2.5.1. Sample preparation

Ulva rigida disks were individually homogenized in a chilled glass mortar and pestle in 500 μl of phosphate saline buffer (PBS: 0.14 M NaCl, 2.7 mM KCl, 8.1 mM Na_2HPO_4, and 1.47 mM KH_2PO_4, pH 7.4). Homogenates were centrifuged at 15,000 x g for 5 min at 4°C and stored at -80°C.

Samples were run in triplicates (technical replicates) and all the results were normalized to total protein content by the method of Lowry et al. (1951).

2.5.2. Antioxidant enzymes

(i) The percentage of inhibition of superoxide dismutase (SOD) was ascertained adapting Sun et al. (1988) method. Concisely, 200 μl of 50 mM phosphate buffer (pH 8.0) (Merck, Germany), 10 μl of 3 mM EDTA (Riedel-de Haën), 10 μl of 3 mM xanthine (Merck), 10 μl of 0.75 mM NBT (Merck) and 10 μl of SOD standard or sample were added to each well of a 96-well microplate (Greiner Bio-one, Germany). Following, 10 μl of 100 mU xanthine-oxidase (XOD, Sigma-Aldrich) was added to begin the reaction and the absorbance was read at 560 nm in a plate reader (Biotek Synergy HTX multi-mode reader, USA). The absorbance was recorded every 2 min for 26 min. SOD (Merck) was used as a standard and positive control, and a negative control included all components (except SOD or sample). SOD activity is expressed as % inhibition mg^{-1} of total protein.

(ii) Catalase (CAT) activity was measured according to the method described in Johansson and Borg (1988). Twenty microliters of a sample, 100 μL of 100 mM potassium phosphate, and 30 μL of methanol were added to each well of a 96-well microplate (Greiner Bio-one, Germany) and incubated for 20 min. Subsequently, 30 μL of potassium hydroxide (10 M KOH) and 30 μL of Purpald Reagent (34.2 mM in 0.5 M HCl) were added, and the plate was incubated for 10 min. Then, 10 μL of potassium metaperiodate (65.2 mM in 0.5 M KOH) was added and incubated for 5 min. The activity was assessed spectrophotometrically at 540 nm, in a microplate reader (Biotek Synergy HTX multi-mode reader, USA). Formaldehyde concentration of the samples was calculated based on a calibration curve (from 0 to 75 μM formaldehyde). The results are presented in nmol min^{-1} mg^{-1} protein.

(iii) Glutathione S-transferase (GST) was determined by adapting a method previously described by Habig et al. (1974), and adapted to 96-well microplates (Greiner Bio-one Germany). Accordingly, 180 μl of substrate solution (100 mM 1-chloro-2,4-dinitrobenzene (CDNB), 200 mM L-glutathione and Dulbecco's PBS), 20 μl sample were included in each well of the microplate and the absorbance was read at 340 nm (Biotek Synergy HTX multi-mode reader, USA) six times, once every minute. Equine liver GST (Merck, Germany) was used as a positive control to validate the assay and GST activity calculated using the molar extinction coefficient for CDNB of 5.3 εμM (μM^{-1} cm^{-1}). The results were expressed according to the total protein of the sample (nmol min^{-1} mg^{-1} total protein).

2.5.3. Cellular oxidative damage

Lipid peroxidation (LIPO) was established by malondialdehyde (MDA) quantification, a by-product of lipid damage, according to the thiobarbituric acid reactive substances (TBARS) assay (Uchiyama and Mihara, 1978). Briefly, 10 μL of each sample, 45 μL of PBS, 12.5 μL of sodium dodecyl sulfate (8.1%), 93.5 μL of trichloroacetic acid (20%, pH 3.5), and 93.5 μL of thiobarbituric acid (1%), were added in a 1.5 mL microtube. A total of 50.5 μL of Milli-Q ultrapure water was added to the microtube, mixed, and incubated in a dry bath (Labnet, USA) at 100°C for 10 min. Afterward, this mixture was cooled on ice. After colling, 62.5 μL of Milli-Q ultrapure water and one hundred and fifty μL of supernatant was added to 96-well microplates, and absorbance was read at 532 nm in a microplate reader (Biotek Synergy HTX multi-mode reader, USA). Malondialdehyde concentrations were calculated based on a calibration curve (0–0.1 μM) using MDA bis (dimethyl acetal) standards.

2.6. Chlorophylls and carotenoids

Chlorophylls were determined through an adaptation of the method described by Arnon (1949). A pool of $n = 3$ disks corresponding approximately to 0.15 g wet weight (ww) of *U. rigida* was extracted in 10 mL of 80% (v/v) acetone (Merck) in glass vials that were protected from light and kept at 4°C for 24 h. Samples were run in triplicates (technical replicates) and the absorbance of the supernatants was measured at 663 nm and 645 nm in a UV-spectrophotometer (Biotek Synergy HTX multi-mode reader, USA). To ascertain total chlorophyll (total Chl), the content of chlorophyll a (Chl a) and chlorophyll b (Chl b) were calculated as by Rodrigues et al. (2021):

$$\text{Chl a } (\mu g\ g^{-1}\ ww) = 12.25\ A_{663} - 2.79\ A_{645}$$

$$\text{Chl b } (\mu g\ g^{-1}\ ww) = 21.5\ A_{645} - 5.10\ A_{663}$$

$$\text{Total Chl } (\mu g\ g^{-1}\ ww) = \text{Chl a} + \text{Chl b}$$

The carotenoid content was measured in the same extract used for chlorophyll a and b estimation by the method of Kirk and Allen (1965). Briefly, the extract was measured at 480 nm and the content was calculated as:

$$\text{Carotenoid } (\mu g\ g^{-1}\ ww) = A_{480} + (0.114\ A_{663}) - (0.638\ A_{645})$$

A = absorbance at each respective wavelength

2.7. Data analysis

Two- and Three-way ANOVAs followed by significant Tukey's pairwise comparisons with Temperature, pH, and Contamination as factors for the outputs La or Gd accumulation, SOD, CAT, GST, LIPO, Total Chlorophyll and Carotenoids in each respective sampling time (two-way for T0, three-way for T1, T3, T7 and T14) were performed to explore significant differences between treatments. A one-way ANOVA was performed to explore differences in La and Gd concentrations in La and Gd exposure treatments, between sampling times.

Analyses were performed at a significance level of 0.05 in InVivoStat, version 4.3.

3. Results

Supplemental Table 1 comprises measured master water parameters and calculated pCO_2 values for every experimental treatment.

3.1. Lanthanum and Gd bioaccumulation and elimination

Lanthanum concentrations (μg g^{-1}, dry weight) in La spiked *U. rigida* are shown in Fig. 1a while Gd concentrations (μg g^{-1}, dry weight) in Gd exposed treatments are shown in Fig. 1b. Table 1 shows median (minimum-maximum) La and Gd concentrations (μg g^{-1}, dry weight) in *U. rigida* samples for every experimental condition. Table 2 presents the La and Gd levels in the water (μg L^{-1}) aliquots sampled after 24 h (immediately before T1) in all experimental treatments.

We observed La accumulation just after 24 h, as the La spiked treatments showcased significant differences from their control counterparts ($p < 0.0001$), and the La accumulation was greater in the Acidification & La treatment than in the Warming, acidification & La one ($p = 0.0022$). On the first day of exposure, the La water levels diminished in the Acidification & La treatment 96% (Table 2), followed by 95% in the La treatment. The La reduction was lowest in the Warming & La treatment (88%), closely followed by the La exposure treatment (89%). Regarding the La trial at T3, the La accumulation was upheld and increased. At T3, La concentrations were significantly lower in the Warming, acidification & La than the other three La exposed treatments ($p < 0.05$). At T7 we only observed significant lower La levels in the Warming, acidification & La than the Warming & La treatment ($p = 0.0152$).

Considering the Gd exposure trial, after one day of exposure, Gd accumulation occurred in all Gd exposed treatments ($p < 0.0001$). The Gd accumulation trend was similar to the La trial. Here the accumulation was greater in the Acidification & Gd treatment than the Gd treatment (p=<0.0001), the Warming & Gd ($p = 0.0004$), and the Warming, acidification & Gd (p=<0.0001). The Gd reduction from water, in the

Table 1
Median, minimum, and maximum La and Gd concentrations (μg g^{-1}, dry weight) in *Ulva rigida* exposed to: control/present-day temperature and pH; Acidification; La; Acidification & La; Gd; Acidification & Gd; Warming; Warming & acidification; Warming & La; Warming & Gd; Warming, acidification & La; Warming, acidification & Gd at T0, T1, T3, T7 and T14. BDL stands for below detection limit. Detection limits were 0.12 μg L^{-1} for La and 0.032 μg L^{-1} for Gd.

	[La] (μg g^{-1} dry weight)				
	T0	T1	T3	T7	T14
Control temperature & pH	BDL	0.12 (0.12-0.18)	0.23 (0.19-0.28)	0.34 (0.28-0.39)	0.20 (0.12-0.24)
Acidification	BDL	0.12 (0.12-0.14)	0.14 (0.12-0.16)	0.16 (0.12-0.20)	BDL
La		10 (7.7-13)	24 (14-27)	40 (37-43)	42 (32-46)
Acidification & La		13 (9.2-15)	30 (21-30)	40 (32-47)	41 (39-50)
Warming	BDL	0.12 (0.12-0.64)	BDL	0.12 (0.12-0.12)	BDL
Warming & Acidification	BDL	BDL	BDL	0.21 (0.20-0.76)	BDL
Warming & La		11 (0.12-12)	25 (23-30)	39 (31-69)	33 (29-49)
Warming, acidification & La		9.2 (7.7-11)	16 (13-19)	29 (27-33)	19 (16-25)
	[Gd] (μg g^{-1} dry weight)				
	T0	**T1**	**T3**	**T7**	**T14**
Control temperature & pH	BDL	0.038 (0.032-0.046)	0.048 (0.032-0.060)	BDL	BDL
Acidification	BDL	0.032 (0.032-0.054)	0.057 (0.043-0.060)	0.064 (0.043-0.11)	0.033 (0.032-0.14)
Gd		4.5 (3.9-5.9)	11 (8.2-12)	22 (19-22)	22 (20-25)
Acidification & Gd		8.4 (6.2-9.0)	15 (12-16)	21 (17-22)	19 (12-28)
Warming	BDL	BDL	0.042 (0.032-0.046)	BDL	BDL
Warming & Acidification	BDL	BDL	BDL	BDL	BDL
Warming & Gd		5.5 (5.4-7.8)	20 (18-21)	24 (20-28)	21 (18-27)
Warming, acidification & Gd		5.3 (4.9-6.2)	10 (9.5-12)	27 (27-28)	26 (22-27)

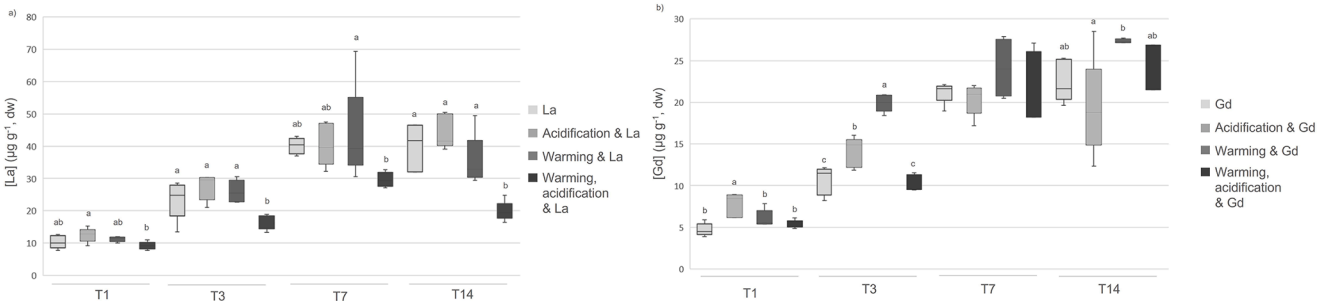

Fig. 1. Median, percentile 25th and 75th, minimum and maximum values of: (a) Lanthanum and (b) gadolinium (μg $^{-1}$) concentrations in *Ulva rigida* exposed to 15 μg L^{-1} and 10 μg L^{-1}, respectively, in different sampling times (T1, T3, T7 and T14). Different letters represent significant differences between exposure treatments within sampling times.

Table 2
Levels of La and Gd in the water (μg L^{-1}) aliquots sampled after 24 h (immediately before T1) of exposure in all experimental treatments.

	[La] (μg L^{-1}) 24 h	[Gd] (μg L^{-1})
Control temperature & pH	0.010	0.004
La	**0.72**	-
Gd	-	**0.60**
Acidification	0.013	0.009
Acidification & La	**0.63**	-
Acidification & Gd	-	**0.76**
Warming	0.008	0.004
Warming & La	**1.8**	-
Warming & Gd	-	**0.74**
Warming & Acidification	0.009	0.004
Warming, acidification & La	**1.7**	-
Warming, acidification & Gd	-	**3.7**

first 24h, was greatest in the Gd exposure treatment 94% (Table 2) followed by the Warming & Gd (93%), the Acidification & Gd treatment (92%). The lowest reduction was exhibited in the Warming, acidification & Gd (63%). At T3, the Gd exposure treatment showed significantly lower accumulation values than the algae exposed to both Warming & Gd ($p < 0.0001$) and Acidification & Gd ($p = 0.0001$). The Warming & Gd also showed significantly higher values than the Acidification & Gd treatment (p=<0.0001). Lastly, the Warming, acidification & Gd treatment showed significantly lower values than the Acidification & Gd and Warming & Gd treatments ($p < 0.0001$ and $p < 0.0001$, respectively). At T7, no differences in Gd accumulation were found between the Gd exposed treatments ($p > 0.05$).

Regarding the elimination phase, 7 days of elimination were insufficient. At T14, every La and Gd exposed treatment remained different than their control counterpart (Supplemental Table 3a). Additionally, the concentration values presented at T14 were very similar to the ones at T7. In fact, from time T7 to T14 we only observed a significant difference in the Warming, acidification & La treatment ($p < 0.0001$). The first sampling time for the La and Gd concentrations in the exposed treatments, respectively, was different from all the other (T1 vs T3, T7, and T14, $p < 0.05$). The La and Gd concentrations in T3 were significantly lower than T7 for all spiked treatments.

Fig. 2 shows the bioaccumulation factor at T7 and the elimination coefficient, for both studied elements. Overall, La exposed Ulva disks showed bioaccumulation factors greater than the ones exposed to Gd, except for specimens exposed under a Warming & Acidification scenario. Greater Gd accumulation values under Warming & Acidification were met by a greater elimination than La.

3.2. Oxidative stress-related biomarkers

Oxidative stress-related biomarkers values for every experimental treatment and time are presented in Table 3.

3.2.1. SOD

The superoxide dismutase (SOD, % inhibition min^{-1} mg^{-1} protein) levels for the exposure treatments of the La and Gd trials are shown in Fig. 3a and b, respectively.

For the La trial, warming induced SOD values, just after one day ($p = 0.0308$). The impacts of climate change on increased SOD values were also visible at T3, and the four La exposure treatments showed enhanced SOD levels in comparison to the control samples (Supplemental Table 3a). At T7, the La exposure treatments remained significantly higher than the control, except for the Acidification & La treatment ($p > 0.05$). Additionally, we observed that La in conjugation with climate change (i.e., Acidification & Warming) triggered an enhanced SOD activity, in comparison to La exposure ($p = 0.0193$ and p=<0.0001). On another hand, the Acidification & La treatment caused diminished SOD values, in comparison to the Acidification treatment ($p = 0.0027$). The

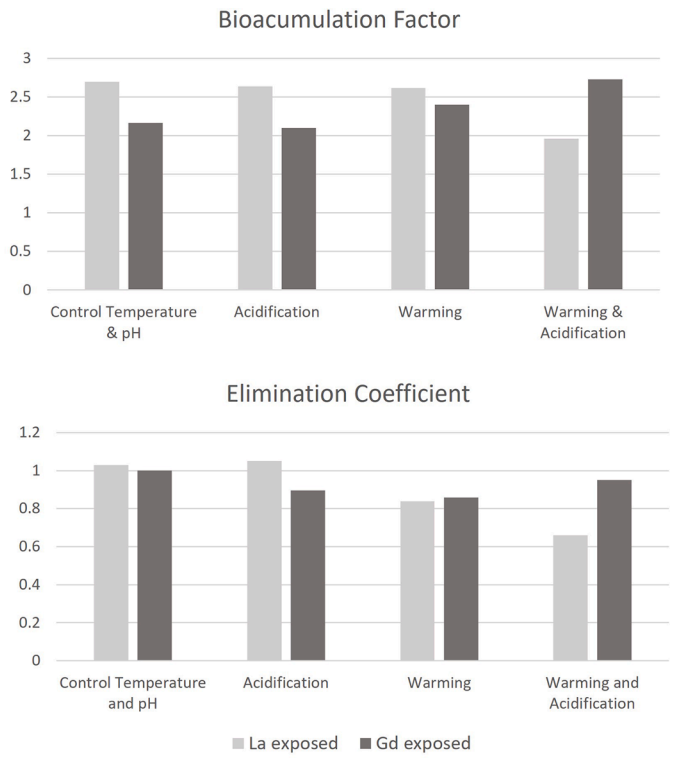

Fig. 2. Bioaccumulation factor at T7 and elimination coefficient for La and Gd exposed treatments

Warming & La treatment provoked significantly higher SOD than the Acidification & La ($p = 0.0007$). At the end of the elimination period (T14), we observed that the treatments Warming & La and Warming, acidification & La displayed enhanced SOD, analogous to the La exposure treatment ($p = 0.0181$ and $p = 0.018$, respectively).

Ulva rigida disks exposed for 24 h to Gd showcased enhanced SOD levels in comparison to the control ($p = 0.0176$) and the Acidification treatments ($p = 0.0027$). In addition, the Acidification & Gd showed higher values than the Acidification treatment ($p = 0.0123$). On the third exposure day, all four Gd exposure treatments showed higher SOD levels than the control (Supplemental Table 3a). Gadolinium exposure caused higher SOD levels than Acidification ($p < 0.0001$), and Warming & acidification combined ($p = 0.0131$). The combination of Acidification & Gd also triggered enhanced SOD levels, in comparison to just Acidification (p=<0.0001). Finally, at T3, SOD levels were greater in Warming, acidification & Gd than in the Warming & acidification treatment ($p = 0.0093$). On the 7th day, all four Gd exposure treatments showed higher SOD than the control ($p < 0.05$). The combination of Warming, acidification & Gd resulted in the highest SOD levelsAt T14, the previously enhanced SOD levels from the four Gd exposure treatments decreased to control-like values, and we did not observe significant differences between experimental treatments.

3.2.2. CAT

Catalase (CAT, nmol min^{-1} mg^{-1} total protein) values for the exposure treatments of the La and Gd trials are shown in Fig. 3 c and d.

On the La trial, significant differences between treatments were only visible at T3 and T14. On the Gd trial, we only observed differences at T3. On T3, *U. rigida* exposed to Acidification & La showed lower CAT levels than the control ($p = 0.0277$). At T14, the previously exposed algae to La, Acidification & La and Warming, acidification & La showed an inhibition of CAT in comparison to the control ($p = 0.008$, $p = 0.0198$, $p = 0.0226$, respectively).

At T3, Acidification & Gd exposure inhibited CAT expression in comparison to the control ($p = 0.0196$) and the warming treatment ($p =$

Table 3
Mean ± standard deviation values of Superoxide dismutase (SOD, % inhibition min^{-1} mg^{-1} protein); Catalase (CAT, nmol min^{-1} mg^{-1} protein); Glutathione S-transferase (GST, nmol min^{-1} mg^{-1} total protein); Lipid peroxidation (LPO, nmol mg protein $^{-1}$); Total Chlorophyll (mg g^{-1}, ww); Carotenoid (mg g^{-1}, ww) in *Ulva rigida* at T0, T1, T3, T7 and T14 in all experimental treatments.

		SOD (% inhibition min^{-1} mg^{-1} protein)	CAT (nmol min^{-1} mg^{-1} protein)	GST (nmol min^{-1} mg^{-1} total protein)	LIPO (nmol mg protein $^{-1}$)	Total Chlorophyll (mg g^{-1}, ww)	Carotenoids (mg g^{-1}, ww)
T0	Control	175 ± 67	1.2 ± 0.04	33 ± 2.7	0.037 ± 0.008	1.3 ± 0.036	0.065 ± 0.004
	Acidification	152 ± 14	1.1 ± 0.20	29 ± 3.8	0.029 ± 0.0002	1.3 ± 0.005	0.077 ± 0.001
	Warming	131 ± 24	1.1 ± 0.22	32 ± 8.0	0.032 ± 0.006	1.3 ± 0.049	0.075 ± 0.002
	Warming & Acidification	134 ± 40	1.1 ± 0.04	39 ± 3.9	0.030 ± 0.004	1.2 ± 0.013	0.058 ± 0.004
T1	Control	181 ± 21	1.2 ± 0.31	38 ± 4.3	0.028 ± 0.008	1.2 ± 0.17	0.055 ± 0.006
	La	293 ± 27	1.4 ± 0.44	49 ± 10	0.034 ± 0.018	1.7 ± 0.025	0.042 ± 0.009
	Gd	336 ± 65	1.6 ± 0.42	55 ± 4.1	0.026 ± 0.014	1.0 ± 0.033	0.043 ± 0.001
	Acidification	184 ± 76	1.2 ± 0.16	30 ± 3.4	0.027 ± 0.015	1.3 ± 0.086	0.051 ± 0.015
	Acidification & La	292 ± 51	1.5 ± 0.37	41 ± 9.0	0.040 ± 0.013	1.4 ± 0.30	0.042 ± 0.0001
	Acidification & Gd	314 ± 84	1.6 ± 0.39	52 ± 4.2	0.039 ± 0.008	0.90 ± 0.010	0.042 ± 0.007
	Warming	361 ± 84	1.3 ± 0.35	36 ± 2.0	0.028 ± 0.007	1.4 ± 0.11	0.045 ± 0.007
	Warming & La	348 ± 90	1.3 ± 0.31	50 ± 6.3	0.059 ± 0.019	1.9 ± 0.73	0.038 ± 0.012
	Warming & Gd	273 ± 92	1.2 ± 0.34	57 ± 3.4	0.044 ± 0.025	1.5 ± 0.030	0.093 ± 0.017
	Warming & acidification	267 ± 58	1.3 ± 0.17	45 ± 3.9	0.031 ± 0.009	1.2 ± 0.65	0.062 ± 0.020
	Warming, acidification & La	212 ± 88	1.0 ± 0.14	50 ± 11	0.056 ± 0.015	2.1 ± 0.34	0.06 ± 0.008
	Warming, acidification & Gd	212 ± 66	1.4 ± 0.05	48 ± 5.4	0.051 ± 0.019	1.6 ± 0.47	0.052 ± 0.005
T3	Control	234 ± 59	1.2 ± 0.30	41 ± 5.2	0.038 ± 0.009	0.90 ± 0.030	0.035 ± 0.0005
	La	341 ± 35	0.66 ± 0.15	45 ± 16	0.067 ± 0.025	1.2 ± 0.060	0.04 ± 0.001
	Gd	486 ± 58	0.51 ± 0.09	53 ± 20	0.06 ± 0.011	1.0 ± 0.022	0.043 ± 0.011
	Acidification	270 ± 24	1.0 ± 0.08	37 ± 8.9	0.051 ± 0.014	1.3 ± 0.080	0.049 ± 0.002
	Acidification & La	336 ± 58	0.54 ± 0.18	46 ± 7.0	0.061 ± 0.038	1.6 ± 0.018	0.060 ± 0.0
	Acidification & Gd	468 ± 21	0.47 ± 0.2	56 ± 7.2	0.066 ± 0.001	1.3 ± 0.083	0.059 ± 0.020
	Warming	404 ± 30	1.0 ± 0.14	52 ± 13	0.067 ± 0.05	1.4 ± 0.042	0.065 ± 0.004
	Warming & La	419 ± 47	0.65 ± 0.1	51 ± 3.5	0.066 ± 0.022	1.6 ± 0.23	0.057 ± 0.010
	Warming & Gd	545 ± 66	0.62 ± 0.21	58 ± 12	0.071 ± 0.012	1.4 ± 0.041	0.054 ± 0.001
	Warming & acidification	370 ± 49	0.92 ± 0.19	42 ± 14	0.056 ± 0.019	1.0 ± 0.045	0.050 ± 0.023
	Warming, acidification & La	439 ± 72	0.71 ± 0.09	55 ± 15	0.068 ± 0.02	2.0 ± 0.036	0.079 ± 0.0002
	Warming, acidification & Gd	491 ± 63	0.6 ± 0.22	45 ± 18	0.074 ± 0.006	1.8 ± 0.025	0.067 ± 0.004
T7	Control	250 ± 15	1.2 ± 0.13	40 ± 5.9	0.036 ± 0.013	1.6 ± 0.026	0.063 ± 0.001
	La	343 ± 66	0.75 ± 0.17	48 ± 11	0.068 ± 0.027	1.6 ± 0.060	0.061 ± 0.002
	Gd	478 ± 49	0.67 ± 0.11	49 ± 5.3	0.08 ± 0.026	1.7 ± 0.077	0.059 ± 0.012
	Acidification	430 ± 54	0.91 ± 0.18	40 ± 5.4	0.056 ± 0.02	1.6 ± 0.32	0.078 ± 0.010
	Acidification & La	305 ± 60	0.66 ± 0.04	37 ± 14	0.073 ± 0.042	1.7 ± 0.098	0.084 ± 0.005
	Acidification & Gd	482 ± 49	0.5 ± 0.12	53 ± 8.0	0.07 ± 0.009	1.6 ± 0.073	0.066 ± 0.007
	Warming	386 ± 48	0.85 ± 0.11	49 ± 12	0.047 ± 0.024	1.5 ± 0.074	0.076 ± 0.004
	Warming & La	453 ± 39	0.73 ± 0.21	47 ± 7.8	0.069 ± 0.028	1.7 ± 0.006	0.067 ± 0.009
	Warming & Gd	575 ± 54	0.74 ± 0.25	85 ± 11	0.083 ± 0.012	1.5 ± 0.31	0.080 ± 0.001
	Warming & acidification	438 ± 90	0.84 ± 0.02	39 ± 2.2	0.05 ± 0.02	1.3 ± 0.018	0.053 ± 0.001
	Warming, acidification & La	585 ± 45	0.56 ± 0.13	65 ± 10	0.077 ± 0.008	1.9 ± 0.054	0.077 ± 0.011
	Warming, acidification & Gd	639 ± 87	0.53 ± 0.18	72 ± 8.8	0.084 ± 0.025	2.0 ± 0.43	0.087 ± 0.011
T14	Control	286 ± 38	1.1 ± 0.15	38 ± 5	0.031 ± 0.004	1.5 ± 0.10	0.059 ± 0.002
	La	259 ± 61	0.56 ± 0.06	38 ± 3.3	0.043 ± 0.028	1.5 ± 0.14	0.056 ± 0.012
	Gd	419 ± 81	0.62 ± 0.11	36 ± 17	0.063 ± 0.002	1.6 ± 0.17	0.063 ± 0.001
	Acidification	342 ± 63	0.94 ± 0.05	38 ± 8.4	0.048 ± 0.033	1.5 ± 0.027	0.057 ± 0.010
	Acidification & La	259 ± 40	0.61 ± 0.15	35 ± 13	0.055 ± 0.013	1.6 ± 0.008	0.077 ± 0.012
	Acidification & Gd	379 ± 16	0.87 ± 0.35	39 ± 4.5	0.056 ± 0.038	1.6 ± 0.24	0.066 ± 0.003
	Warming	361 ± 43	0.92 ± 0.42	33 ± 6.9	0.059 ± 0.02	1.7 ± 0.008	0.057 ± 0.005
T14	Warming & La	415 ± 110	0.69 ± 0.23	33 ± 5.4	0.058 ± 0.03	1.4 ± 0.013	0.062 ± 0.006
	Warming & Gd	440 ± 116	0.82 ± 0.13	82 ± 4.6	0.062 ± 0.023	1.7 ± 0.098	0.067 ± 0.004
	Warming & acidification	375 ± 41	0.85 ± 0.08	32 ± 10	0.059 ± 0.013	1.4 ± 0.16	0.061 ± 0.002
	Warming, acidification & La	401 ± 124	0.61 ± 0.13	54 ± 9.0	0.048 ± 0.023	1.7 ± 0.52	0.081 ± 0.007
	Warming, acidification & Gd	402 ± 61	0.82 ± 0.41	58 ± 17	0.064 ± 0.05	1.8 ± 0.011	0.072 ± 0.001

0.0331).

3.2.3. GST

Glutathione S-transferase (GST, nmol min^{-1} mg^{-1} total protein) levels for the exposure treatments of the La and Gd experiments, and their respective controls, are presented in Fig. 3e and f, respectively.

At T1, the combination of La and climate change variables synergistically enhanced GST expression (Fig. 2e). Acidification & La exposure prompted higher GST levels than Acidification exposure (p = 0.0443) and Warming & La prompted higher levels than Warming as a

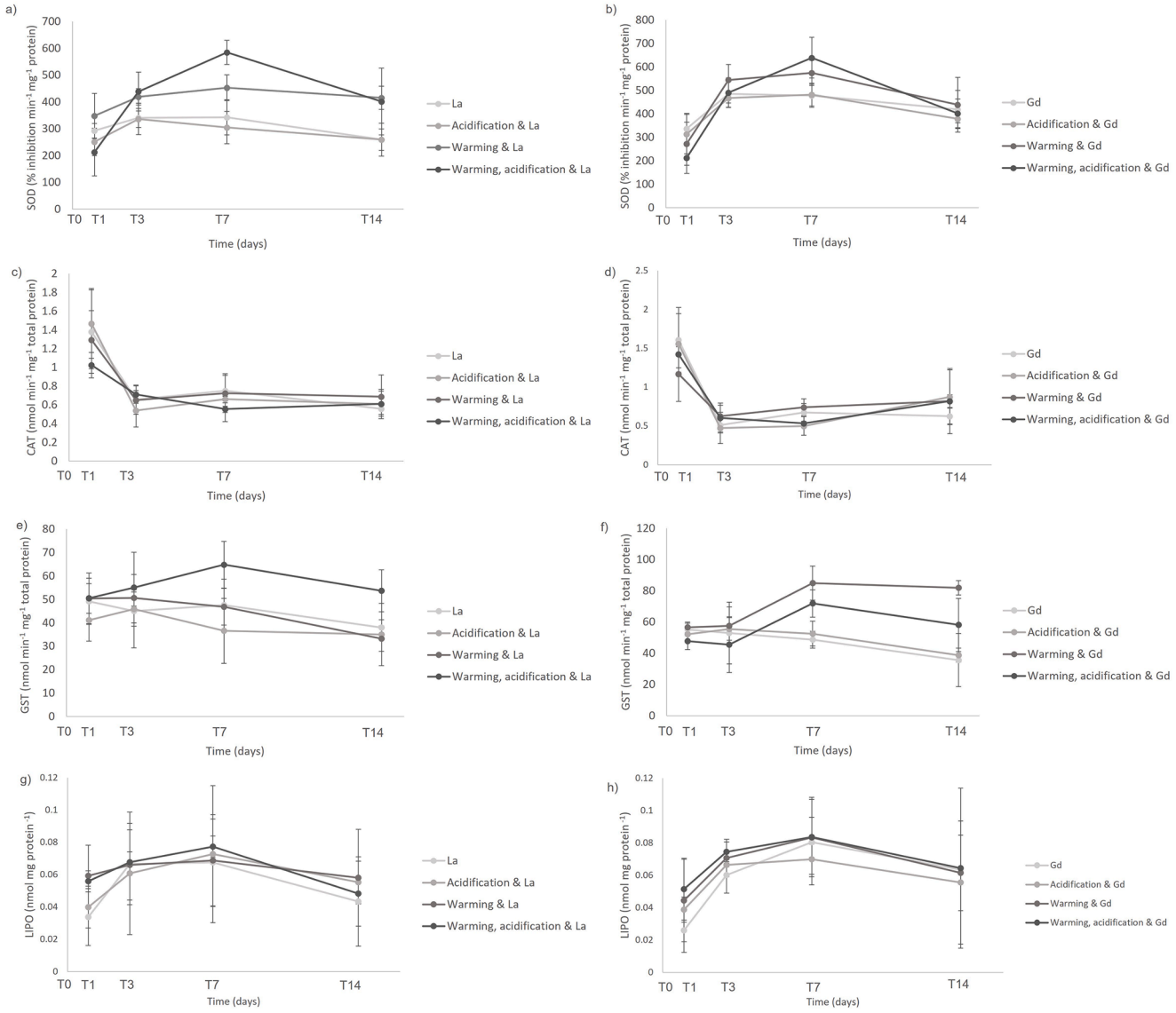

Fig. 3. Mean ± SD values of: Superoxide dismutase (SOD, % inhibition min^{-1} mg^{-1} protein); (CAT, nmol min^{-1} mg^{-1} protein); Glutathione S-transferase (GST, nmol min^{-1} mg^{-1} total protein) and Lipid peroxidation (LIPO, nmol mg protein $^{-1}$) in *Ulva rigida*'s disks at T1, T3, T7 and T14. (a), (c), (d) and (g) represent the La exposure trial and (b), (d), (f) and (h) represent the Gd exposure trial.

single stressor ($p = 0.0244$). Furthermore, Warming, Acidification & La showed increased levels than Warming ($p = 0.0166$). After 7 days of exposure to the combination of Warming, acidification & La, *U. rigida* specimens presented significantly higher GST values than specimens exposed to Acidification & La ($p = 0.0032$) and Acidification ($p = 0.014$). After the elimination period (T14), the enhanced GST levels triggered by the exposure to Warming, Acidification & La decreased slightly and remained the highest, being significantly higher than the Warming ($p = 0.0317$), Warming & La ($p = 0.0317$), and Warming & Acidification ($p = 0.0106$).

After just one day of exposure (T1) all the Gd exposure treatments showcased significantly higher GST values than the control ($p < 0.05$). Furthermore, Gd exposure triggered higher GST expression than Acidification (p=<0.0001) and Warming ($p < 0.0001$). The Acidification & Gd also showed higher GST levels than Acidification alone ($p < 0.0001$) while Warming & Gd showed higher GST levels than Warming alone ($p < 0.0001$). Warming, acidification & Gd triggered enhanced GST expression in comparison to Warming ($p = 0.0017$) and Acidification (p=<0.0001). At T7, Warming & Gd elicited enhanced GST values, in comparison to the control ($p = 0.0004$), to the Gd exposure ($p = 0.0049$), and the Warming treatment ($p = 0.0012$). Moreover, Warming, acidification & Gd prompted greater GST levels than the control ($p = 0.0112$), and the Warming & acidification treatment ($p = 0.0076$). At the end of the elimination phase, the GST values presented by the *U. rigida* exposed to Warming & Gd remained significantly higher than those found in the control ($p = 0.0004$) and the Gd exposure treatment ($p = 0.0001$). At this time, T14, Warming, Acidification & Gd showed significantly greater GST values than Warming & Acidification ($p = 0.0027$), Warming ($p = 0.0093$), and Gd exposure treatment ($p = 0.0376$).

3.2.4. LIPO

Lipid peroxidation (LIPO, nmol mg $protein^{-1}$) levels in *U. rigida* samples exposed to La and Gd, in present-day and predicted climate change conditions are shown in Fig. 3g and h, respectively.

Although we did not observe significant differences in the LIPO levels between the exposure treatments, along the experimental times the levels increased from T1 to T3 ($p = 0.0493$) and T7 ($p = 0.0141$) in the Gd exposure treatment and from T1 to T7 ($p = 0.0441$) in the Acidification & Gd treatment.

3.3. Total chlorophyll and carotenoid content

Contents of total chlorophyll and carotenoids are given in Table 4. Levels for the exposure treatments of the La and Gd trials are illustrated in Fig. 4a-d.

At T0, the algae samples acclimated to Warming & acidification showed significantly lower chlorophyll values than the ones kept in control conditions ($p = 0.0305$; Fig. 3a). At T1the four La exposure treatments presented significantly higher total chlorophyll values than the control ($p < 0.05$). The highest chlorophyll content was registered in

Table 4
Mean ± standard deviation values of Superoxide dismutase (SOD, % inhibition min^{-1} mg^{-1} protein); Catalase (CAT, nmol min^{-1} mg^{-1} protein); Glutathione S-transferase (GST, nmol min^{-1} mg^{-1} total protein); Lipid peroxidation (LPO, nmol mg protein $^{-1}$); Total Chlorophyll (mg g^{-1}, ww); Carotenoids (mg g^{-1}, ww) in *Ulva rigida* at T0, T1, T3, T7 and T14 in all experimental treatments.

		SOD (% inhibition min^{-1} mg^{-1} protein)	CAT (nmol min^{-1} mg^{-1} protein)	GST (nmol min^{-1} mg^{-1} total protein)	LIPO (nmol mg protein $^{-1}$)	Total Chlorophyll (mg g^{-1}, ww)	Carotenoids (mg g^{-1}, ww)
T0	Control	175 ± 67	1.2 ± 0.04	33 ± 2.7	0.037 ± 0.008	1.3 ± 0.036	0.065 ± 0.004
	Acidification	152 ± 14	1.1 ± 0.20	29 ± 3.8	0.029 ± 0.0002	1.3 ± 0.005	0.077 ± 0.001
	Warming	131 ± 24	1.1 ± 0.22	32 ± 8.0	0.032 ± 0.006	1.3 ± 0.049	0.075 ± 0.002
	Warming & Acidification	134 ± 40	1.1 ± 0.04	39 ± 3.9	0.030 ± 0.004	1.2 ± 0.013	0.058 ± 0.004
T1	Control	181 ± 21	1.2 ± 0.31	38 ± 4.3	0.028 ± 0.008	1.2 ± 0.17	0.055 ± 0.006
	La	293 ± 27	1.4 ± 0.44	49 ± 10	0.034 ± 0.018	1.7 ± 0.025	0.042 ± 0.009
	Gd	336 ± 65	1.6 ± 0.42	55 ± 4.1	0.026 ± 0.014	1.0 ± 0.033	0.043 ± 0.001
	Acidification	184 ± 76	1.2 ± 0.16	30 ± 3.4	0.027 ± 0.015	1.3 ± 0.086	0.051 ± 0.015
	Acidification & La	292 ± 51	1.5 ± 0.37	41 ± 9.0	0.040 ± 0.013	1.4 ± 0.30	0.042 ± 0.0001
	Acidification & Gd	314 ± 84	1.6 ± 0.39	52 ± 4.2	0.039 ± 0.008	0.90 ± 0.010	0.042 ± 0.007
	Warming	361 ± 84	1.3 ± 0.35	36 ± 2.0	0.028 ± 0.007	1.4 ± 0.11	0.045 ± 0.007
	Warming & La	348 ± 90	1.3 ± 0.31	50 ± 6.3	0.059 ± 0.019	1.9 ± 0.73	0.038 ± 0.012
	Warming & Gd	273 ± 92	1.2 ± 0.34	57 ± 3.4	0.044 ± 0.025	1.5 ± 0.030	0.093 ± 0.017
	Warming & acidification	267 ± 58	1.3 ± 0.17	45 ± 3.9	0.031 ± 0.009	1.2 ± 0.65	0.062 ± 0.020
	Warming, acidification & La	212 ± 88	1.0 ± 0.14	50 ± 11	0.056 ± 0.015	2.1 ± 0.34	0.06 ± 0.008
	Warming, acidification & Gd	212 ± 66	1.4 ± 0.05	48 ± 5.4	0.051 ± 0.019	1.6 ± 0.47	0.052 ± 0.005
T3	Control	234 ± 59	1.2 ± 0.30	41 ± 5.2	0.038 ± 0.009	0.90 ± 0.030	0.035 ± 0.0005
	La	341 ± 35	0.66 ± 0.15	45 ± 16	0.067 ± 0.025	1.2 ± 0.060	0.04 ± 0.001
	Gd	486 ± 58	0.51 ± 0.09	53 ± 20	0.06 ± 0.011	1.0 ± 0.022	0.043 ± 0.011
	Acidification	270 ± 24	1.0 ± 0.08	37 ± 8.9	0.051 ± 0.014	1.3 ± 0.080	0.049 ± 0.002
	Acidification & La	336 ± 58	0.54 ± 0.18	46 ± 7.0	0.061 ± 0.038	1.6 ± 0.018	0.060 ± 0.0
	Acidification & Gd	468 ± 21	0.47 ± 0.2	56 ± 7.2	0.066 ± 0.001	1.3 ± 0.083	0.059 ± 0.020
	Warming	404 ± 30	1.0 ± 0.14	52 ± 13	0.067 ± 0.05	1.4 ± 0.042	0.065 ± 0.004
	Warming & La	419 ± 47	0.65 ± 0.1	51 ± 3.5	0.066 ± 0.022	1.6 ± 0.23	0.057 ± 0.010
	Warming & Gd	545 ± 66	0.62 ± 0.21	58 ± 12	0.071 ± 0.012	1.4 ± 0.041	0.054 ± 0.001
	Warming & acidification	370 ± 49	0.92 ± 0.19	42 ± 14	0.056 ± 0.019	1.0 ± 0.045	0.050 ± 0.023
	Warming, acidification & La	439 ± 72	0.71 ± 0.09	55 ± 15	0.068 ± 0.02	2.0 ± 0.036	0.079 ± 0.0002
	Warming, acidification & Gd	491 ± 63	0.6 ± 0.22	45 ± 18	0.074 ± 0.006	1.8 ± 0.025	0.067 ± 0.004
T7	Control	250 ± 15	1.2 ± 0.13	40 ± 5.9	0.036 ± 0.013	1.6 ± 0.026	0.063 ± 0.001
	La	343 ± 66	0.75 ± 0.17	48 ± 11	0.068 ± 0.027	1.6 ± 0.060	0.061 ± 0.002
	Gd	478 ± 49	0.67 ± 0.11	49 ± 5.3	0.08 ± 0.026	1.7 ± 0.077	0.059 ± 0.012
	Acidification	430 ± 54	0.91 ± 0.18	40 ± 5.4	0.056 ± 0.02	1.6 ± 0.32	0.078 ± 0.010
	Acidification & La	305 ± 60	0.66 ± 0.04	37 ± 14	0.073 ± 0.042	1.7 ± 0.098	0.084 ± 0.005
	Acidification & Gd	482 ± 49	0.5 ± 0.12	53 ± 8.0	0.07 ± 0.009	1.6 ± 0.073	0.066 ± 0.007
	Warming	386 ± 48	0.85 ± 0.11	49 ± 12	0.047 ± 0.024	1.5 ± 0.074	0.076 ± 0.004
	Warming & La	453 ± 39	0.73 ± 0.21	47 ± 7.8	0.069 ± 0.028	1.7 ± 0.006	0.067 ± 0.009
	Warming & Gd	575 ± 54	0.74 ± 0.25	85 ± 11	0.083 ± 0.012	1.5 ± 0.31	0.080 ± 0.001
	Warming & acidification	438 ± 90	0.84 ± 0.02	39 ± 2.2	0.05 ± 0.02	1.3 ± 0.018	0.053 ± 0.001
	Warming, acidification & La	585 ± 45	0.56 ± 0.13	65 ± 10	0.077 ± 0.008	1.9 ± 0.054	0.077 ± 0.011
	Warming, acidification & Gd	639 ± 87	0.53 ± 0.18	72 ± 8.8	0.084 ± 0.025	2.0 ± 0.43	0.087 ± 0.011
T14	Control	286 ± 38	1.1 ± 0.15	38 ± 5	0.031 ± 0.004	1.5 ± 0.10	0.059 ± 0.002
	La	259 ± 61	0.56 ± 0.06	38 ± 3.3	0.043 ± 0.028	1.5 ± 0.14	0.056 ± 0.012
	Gd	419 ± 81	0.62 ± 0.11	36 ± 17	0.063 ± 0.002	1.6 ± 0.17	0.063 ± 0.001
	Acidification	342 ± 63	0.94 ± 0.05	38 ± 8.4	0.048 ± 0.033	1.5 ± 0.027	0.057 ± 0.010
	Acidification & La	259 ± 40	0.61 ± 0.15	35 ± 13	0.055 ± 0.013	1.6 ± 0.008	0.077 ± 0.012
	Acidification & Gd	379 ± 16	0.87 ± 0.35	39 ± 4.5	0.056 ± 0.038	1.6 ± 0.24	0.066 ± 0.003
	Warming	361 ± 43	0.92 ± 0.42	33 ± 6.9	0.059 ± 0.02	1.7 ± 0.008	0.057 ± 0.005
	Warming & La	415 ± 110	0.69 ± 0.23	33 ± 5.4	0.058 ± 0.03	1.4 ± 0.013	0.062 ± 0.006
	Warming & Gd	440 ± 116	0.82 ± 0.13	82 ± 4.6	0.062 ± 0.023	1.7 ± 0.098	0.067 ± 0.004
	Warming & acidification	375 ± 41	0.85 ± 0.08	32 ± 10	0.059 ± 0.013	1.4 ± 0.16	0.061 ± 0.002
	Warming, acidification & La	401 ± 124	0.61 ± 0.13	54 ± 9.0	0.048 ± 0.023	1.7 ± 0.52	0.081 ± 0.007
	Warming, acidification & Gd	402 ± 61	0.82 ± 0.41	58 ± 17	0.064 ± 0.05	1.8 ± 0.011	0.072 ± 0.001

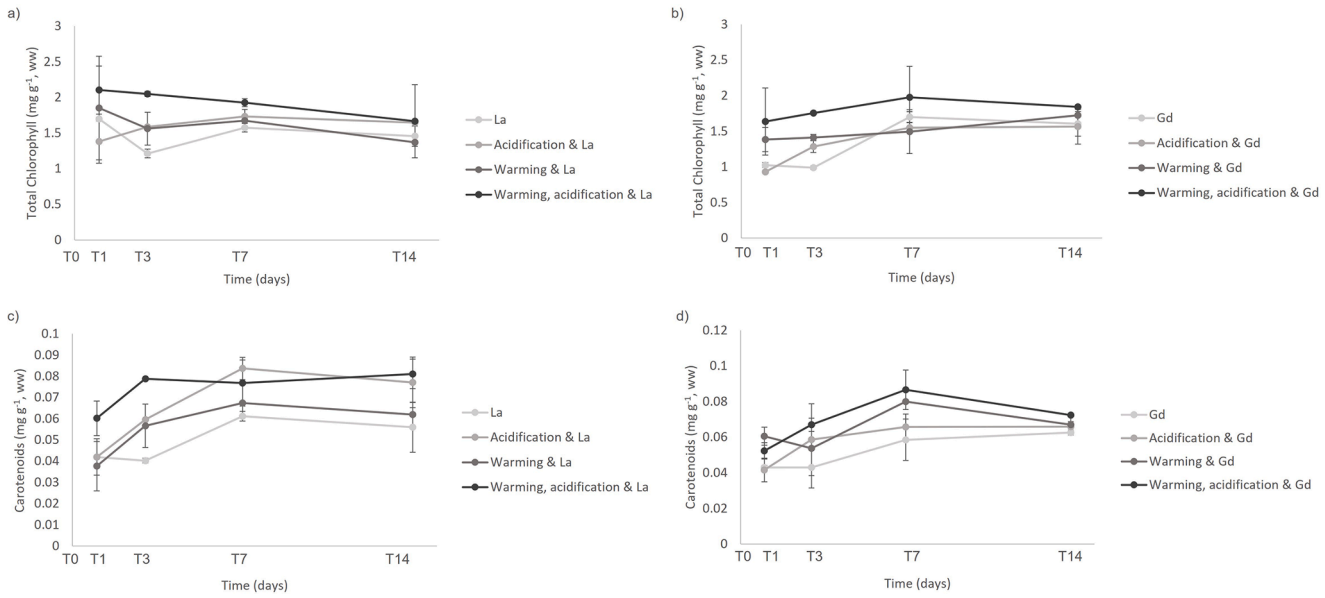

Fig. 4. Mean ± SD values of Total Chlorophyll (mg g^{-1}, ww) and Carotenoid content (mg g^{-1}, ww) in *Ulva rigida* at T1, T3, T7 and T14 in the La (a and c) and Gd (b and d) trials for the four La and Gd exposed treatments, respectively.

U. rigida disks exposed to Warming, acidification & La, and these were significantly greater than the values presented by all the other treatments ($p < 0.05$). T1 showed higher total chlorophyll values than at T3 ($p = 0.0006$) and T14 ($p = 0.0479$). On the contrary, T3 showed significantly lower values than T7 ($p = 0.0029$) and T14 ($p = 0.0253$). At T7, Warming, acidification & La evoked greater chlorophyll content than Warming & acidification ($p = 0.0041$).

Regarding the Gd trial, at T1, Acidification & Gd showed lower total chlorophyll content than Warming & acidification ($p = 0.0278$; Fig. 3b). At T3, Gd exposure in conjugation with climate change variables acting alone and together elicited increased chlorophyll content in comparison to the control ($p < 0.05$), but not Gd exposure alone. While Gd exposure alone revealed greater chlorophyll content than Acidification & Gd ($p = 0.0001$), Warming & Gd exposure triggered greater values than Gd exposure alone ($p < 0.0001$). Alike the La trial, exposure to the three stressors, Warming, acidification & Gd caused enhanced chlorophyll content in comparison to the remaining treatments ($p < 0.05$).

At T3, Acidification & La showed a greater carotenoid content than the control ($p = 0.0178$), while the Warming, acidification & La elicited enhanced carotenoid content than the control ($p = 0.0015$) and the La exposure alone ($p = 0.0065$). At T7, these three stressors in combination (Warming, Acidification & La), caused increased carotenoid content than Warming & acidification ($p = 0.0273$).

Significant differences in carotenoid content of the Gd exposure trial were only found at T7 (Fig. 3d). Here, Warming, acidification & Gd elicited greater carotenoid values than the Gd exposure alone ($p = 0.0375$) and Warming & acidification ($p = 0.0116$).

4. Discussion

Here we showed *U. rigida*'s ability to uptake La and Gd, in mono-element exposure trials, at great levels. Macroalgae are known to significantly bioaccumulate pollutants (e.g., Bonanno et al., 2020), and recent attention has been given to their role in REE removal (Cao et al., 2021), although scarce data on macroalgae interaction with REE is still available. Furthermore, a study encompassing exposure to various stressors related to climate change, such as ocean warming and acidification, and REE with this bioindicator species, has never been carried out.

The literature describes two distinct processes for elemental uptake by algae: i) adsorption onto the cell wall and ii) intracellular absorption (Davis et al., 2003). Although the used methodology is not able to differentiate the two processes, it was clear that one day of exposure proved to be sufficient for La and Gd to be accumulated/adsorbed. *Ulva rigida* exposed to Warming, acidification & La showed the overall lowest accumulation values, while this trend was not observed for Gd, highlighting that although REE are known to be strongly related, displaying a similar chemical behavior, and forming the largest chemically coherent group (Haxel, 2002), the studied elements show different uptake patterns, under future climate-change conditions. Future climate change conditions may interfere with REE uptake patterns as Figueiredo et al. (2020) described enhanced La accumulation in warming scenario for a fish species (*Anguilla anguilla*) and Andrade et al. (2022) described significantly different Gd accumulation values at different salinities (20, 30, and 40) in the mussel *Mytilus galloprovincialis*. Nevertheless, the assessment of single climate change effectson REE is very limited and the absence of information on the combined effects of ocean warming and acidification on REE highlights the urgent need for further studies to be conducted on a wider array of model species in forecasted climate change scenarios.

The green *U. rigida* presents a lobed laminar foliaceous thallus, that encompasses two cell layers (Olivares et al., 2016), which brands this algae species to present a large surface area in contact with seawater. This may have contributed to the great REE accumulation ability shown in this study. Previous studies found distinct accumulation patterns to be related to different algae physical characteristics (e.g., Pinto et al., 2021). Nevertheless, Ferreira et al. (2020) studied the Gd accumulation (10, 157 and 500 μg L^{-1}) using three different marine macroalgae (e.g., *Ulva lactuca, Fucus spiralis* and *Gracilaria* sp.), for 72 h, and all accumulated Gd, with a removal efficiency of around 85%. Moreover, when exposed to a mixture of REE (Y, La, Ce, Pr, Nd, Eu, Tb, Dy) and other elements (Cr, Ni, Cu, Cd, Hg, Pb), at salinity 10 and 30, the removal efficiency was kept (~84%). As expected in the present study, for the same exposure concentration (10 μg L^{-1}), we observed lower uptake percentages, that are likely related do the distinct sampling times (24 h vs 72 h).

The pH is key for REE adsorption onto algae as this is highly dependent on the speciation and the projected pH decrease by the end of the century appears to increase both La and Gd accumulation. As discussed by Cao et al. (2021), REE mostly exist as positively charged ions

and thus exhibit electrostatic attraction towards the negatively charged constituents of the algae surface. When the pH is lower in solution than inside the algae, the REE sorption is obstructed, when the solution pH is higher electrostatic attraction occurs and algae may absorb REE. This may be related to REE speciation shifts, which in turn are regulated by pH, water hardness, alkalinity, ionic strength, and complexing agents (reviewed in Herrmann et al., 2016). In fact, in a previous study we observed La and Gd speciation shifts in fresh-, brackish and saltwater. Increasing ionic strength gave rase to the availability of other complexes than the free ions (La3+ and Gd3+). Furthermore, the La levels were impacted by increasing temperatures and acidification at salinity 15, unlike the Gd levels. The speciation regulates the solubility and bioavailability of an element and therefore underlying differences between the two elements could lead to distinct accumulation and ecotoxicological results. Furthermore, this highpoint that the study of the metal speciation during the exposure phase should be included in upcoming studies. In the present study, accumulation did not stabilize and kept increasing until T7 suggesting that future research should increase the exposure duration, without disregarding frequent sampling of biological material and quantification of REE levels in the water.

The literature reveals a great information gap on REE elimination in macroalgae. Most research focus on REE recycling using micro and macroalgae (e.g. Jacinto et al., 2018), nevertheless, the study of REE elimination by these organisms has been majorly overlooked. Here we showed that neither La nor Gd were eliminated in a 7-day elimination period. In fact, the La and Gd concentrations measured only diminished between T7 and T14 for the Warming, acidification & La treatment. Both climate change stressors combined, Warming and Acidification, contributed to the lowest La accumulation values, in all exposure times and appear to increase La elimination, but not Gd. Here we showed that in a future climate change scenario a different accumulation and elimination pattern between the LREE La and the HREE Gd occurs. As seen in Fig. 2, exposure under the combination of Warming & Acidification induced greater Gd accumulation and elimination, unlike the other experimental treatments. To the best of our knowledge, this is the first assessment on the combined effects of Warming and Acidification on REE accumulation and elimination, which hampers comparison with the literature. Even though the REE are known to behave uniformly and form a chemically coherent group due to the lanthanide contraction, as the radii of elements decreases continuously with increasing atomic number (Hu et al., 2017), this result shows that near future abiotic conditions may alter the biochemical behavior of LREE and HREE. This distinct accumulation and elimination pattern may be related to the previously discussed speciation of both elements, as climate change appears to affect differently the La and Gd species availability (Figueiredo et al., 2022).

Exposure to single and multiple stressors, as climate change and emergent pollutants, is expected to increase the production of reactive oxygen species (ROS). The presence of ROS induces a set of defence mechanisms towards preventing the establishment or neutralizing oxidizing species. When this defence mechanisms fail, the structure and functionality of cells is compromised. For example, if a cell membrane is oxidized by ROS, its rigidity and permeability may be altered with profound consequences to its functionality. Superoxide dismutase (SOD) and catalase (CAT) are the first enzymatic antioxidant's reaction towards ROS. Glutathione-S-transferases (GST) constitute a second line non-enzymatic antioxidant response. In these processes, malondialdehyde is produced and this is used as a biomarker of oxidative stress as an indicator of lipid peroxidation (LIPO).

Higher antioxidant activity levels have been described in *U. rigida* exposed to heavy metals. Olivares et al. (2016) described enhanced antioxidant activity in this algae species in areas with great mining activities. In addition to the antioxidant system, *Ulva* spp. can respond to environmental stress by morphological acclimation (Gao et al., 2016, 2017) and thus future studies on REE ecotoxicity to these species should further detail morphological changes.

Positive effects of REE in algae have been described (Goecke et al., 2015). REE are applied in agriculture and have shown to, for example, increase crop productivity (reviewed by Tyler 2004). However, these results are still not completely clear as several toxic outcomes from REE exposure have similarly been described. Joonas et al. (2017) described the toxic effects of REE on the green microalgae *Raphidocelis subcapitata* and observed growth inhibition within 72 h. Suitable concentrations of REE have been described to increase SOD, and CAT levels, together with higher content of carotenoids, increasing plants' resistance to abiotic stressors, to a threshold as excessive concentration have caused damage to chloroplasts (reviewed in Kovaříková et al., 2019). In fact, Ippolito et al. (2010) described enhanced antioxidant enzymatic responses and glutathione activity in the common duckweed, *Lemna minor* exposed to REE before signs of stress symptoms were observed. A biphasic effect was noted, from antioxidant defence mechanism activation to growth inhibition.

In the present study, exposure to La and Gd triggered the activation of the antioxidant defence system. The response of this system seems to be quicker in the case of Gd exposure, however, on the third day of exposure the four La exposed treatments and the four Gd exposed treatments showed enhanced SOD levels. Furthermore, we observed that this response was higher when the studied REE were combined with climate change variables. The CAT response appeared to be reduced when La and Gd were spiked in an acidification scenario. This is not in line with the response of *Ulva* sp. to other metals as Pereira et al. (2009) showed enhanced CAT activity in specimens environmentally exposed to greater Cu and Ni concentrations. This may be related to a REE specific response. Furthermore, a second line response was activated, highlighted by increased GST levels in REE exposed treatments. Overall, the levels were greater in algae exposed to Warming, Acidification & La, in the La trial while being greater in algae exposed to Warming & Gd, followed by Warming, Acidification & Gd (Gd trial). This response shows that REE exposure in a near future scenario triggers an overproduction of ROS that requests a superior antioxidant response, which in turn may compromise energy requirements and overall species fitness. This response appears to be adequate in avoiding lipid damage as LIPO activity revealed no significant differences. Nevertheless, we observed a trend for greater LIPO values in exposed algae to La and Gd and for that we advise future studies to increase the number of samples studied as we encounter great variability. Furthermore, a broader set of environmentally realistic exposure concentrations may be applied as a previously discussed biphasic effect may occur with increasing concentrations.

This intertidal species shows an extraordinary adaptation ability. In the present study we observed increased total chlorophyll in REE exposure treatments, particularly when combined with climate change, after 3 days of exposure. This was not so obvious on T7 and T14 probably due to this species' previously discussed outstanding adaptation capacity. Nevertheless, an increase in chlorophyll a, chlorophyll b and carotenoids could indicate an unforeseen energy expense to the biosynthesis of pigments, at the cost of growth and reproduction, as a response to a multi-stressor environment. In fact, Ashraf et al. (2021) studied the effects of nanomolar La concentrations on the freshwater green microalga *Desmodesmus quadricauda* and observed that La had no direct effects on growth, but increasing concentrations led to decrease in cell number, and La also inhibited photosynthesis with posterior consequences on growth. Furthermore, La^{3+} is known to precipitate as a phosphate in water, which may lead to phosphorus reduction, that is vital for algae growth, reproduction an ultimately survival (González et al., 2015). Ngwenya et al. (2009) described that heavy REE, such as Gd, are more prone to carboxylate, in this sense exacerbated La concentrations may stand a harsher toxicological threat than Gd to algae species.

In the environment, REE often occur together, and some studies have tried to understand the interaction between mixtures of REE and macroalgae. Jacinto et al. (2018) studied the REE removal ability of red

seaweed *Gracilaria gracilis* by exposing them to mono- and multi-elements REE solutions (Y, Ce, Nd, Eu and La) and observed up to 70% removal in 48h. Removal was greater in multi elemental exposure trials; however, selectivity was not observed. Costa et al. (2020) studied if the presence of Cd, Cr, Cu, Pb, Hg and Ni, interferes with the ability of macroalgae (*Ulva intestinalis, Ulva lactuca, Fucus spiralis, Fucus vesiculosus, Gracilaria* sp. and *Osmundea pinnatifida*) to remove REE (La, Ce, Pr, Nd, Eu, Gd, Tb, Dy and Y) and found that competition of REE to macroalgae sorption sites was minor. Hence, the REE accumulation in mono and multi elemental exposure trials does not seem to be significantly different. Furthermore, the understanding of mono-elemental exposure is still limited, and this study constitutes a great contribution to lessen the knowledge gap regarding the REE individual behavior while starting to unveil their combined effects to a near future setting.

5. Conclusion

The present study is the first assessment of the impacts of ocean warming and acidification on La and Gd accumulation and elimination, through mono-elemental exposure in a factorial design on the green tidal forming *U. rigida* through quantification of an array of non- and enzymatic antioxidant responses and total chlorophyll and carotenoid contents. Overall, we observed distinct La and Gd accumulation patterns in future climate-change conditions and showed that La and Gd are not proficiently eliminated. The exposure to La and Gd triggered the activation of the antioxidant defence system, and this response seems to be quicker in the case of Gd exposure. The response also appears to be adequate in avoiding lipid damage. In a near-future scenario, REE exposure overproduces ROS, which engenders the need for a superior antioxidant response, which may enhance energy requirements with downstream impacts to species fitness.

CRediT authorship contribution statement

Cátia Figueiredo: Conceptualization, Methodology, Validation, Formal analysis, Investigation, Writing – original draft, Funding acquisition. **Tiago F. Grilo:** Conceptualization, Methodology, Validation, Resources, Writing – review & editing, Funding acquisition. **Rui Oliveira:** Conceptualization, Validation, Investigation, Writing – review & editing, Funding acquisition. **Inês João Ferreira:** Methodology, Validation, Writing – review & editing. **Fátima Gil:** Validation, Writing – review & editing. **Clara Lopes:** Validation, Writing – review & editing. **Pedro Brito:** Validation, Writing – review & editing. **Pedro Ré:** Conceptualization, Validation, Resources, Writing – review & editing. **Miguel Caetano:** Conceptualization, Validation, Investigation, Resources, Writing – review & editing, Funding acquisition. **Mário Diniz:** Conceptualization, Validation, Resources, Writing – review & editing, Funding acquisition. **Joana Raimundo:** Conceptualization, Validation, Resources, Writing – review & editing, Funding acquisition.

Declaration of Competing Interest

The authors declare that they have no known competing financial interests or personal relationships that could have appeared to influence the work reported in this paper.

Acknowledgements

This work was supported by Fundação para a Ciência e Tecnologia (FCT), through the project Climatoxeel (PTDC/AAG-GLO/3795/2014) and the Junior Researcher contract (CEECIND/03517/2017), both awarded to Tiago F. Grilo, by the European Union's operation program Mar 2020 through the research project CEIC (MAR-01.04.02-FEAMP-0012) awarded to Joana Raimundo and the strategic project UID/MAR/04292/2019 granted to MARE and by the Applied Molecular Biosciences Unit UCIBIO financed by national funds from FCT (UIDP/04378/2020 and UIDB/04378/2020). Inês João Ferreira acknowledges the European Union research grant ERC-2016-COG-725034-ecotox. Cátia Figueiredo acknowledges the FCT-PhD grant SFRH/BD/130023/2017 and the Early Career Research Grant awarded by National Geographic Society.

Finally, the authors thank the two anonymous reviewers for the many useful comments and valuable advice for the improvement of this work.

Supplementary materials

Supplementary material associated with this article can be found, in the online version, at doi:10.1016/j.envadv.2022.100235.

References

Andrade, M., Soares, A.M., Solé, M., Pereira, E., Freitas, R., 2022. Will climate changes enhance the impacts of e-waste in aquatic systems? Chemosphere 288, 132264.
Arnon, D.I., 1949. Copper enzymes in isolated chloroplasts. Polyphenoloxidase in Beta vulgaris. Plant Physiol. 24 (1), 1.
Ashraf, N., Vítová, M., Cloetens, P., Mijovilovich, A., Bokhari, S.N.H., Küpper, H., 2021. Effect of nanomolar concentrations of lanthanum on Desmodesmus quadricauda cultivated under environmentally relevant conditions. Aquat. Toxicol. 235, 105818.
Åström, M., 2001. Abundance and fractionation patterns of rare earth elements in streams affected by acid sulphate soils. Chem. Geol. 175, 249–258.
Atwood, D.A., 2013. The Rare Earth Elements: Fundamentals and Applications. John Wiley & Sons.
Binnemans, K., McGuiness, P., Jones, P.T., 2021. Rare-earth recycling needs market intervention. Nat. Rev. Mater. 6, 459–461.
Bonanno, G., Veneziano, V., Raccuia, S.A., Orlando-Bonaca, M., 2020. Seagrass Cymodocea nodosa and seaweed Ulva lactuca as tools for trace element biomonitoring. A comparative study. Mar. Pollut. Bull. 161, 111743.
Brito, P., Mil-Homens, M., Caçador, I., Caetano, M., 2020. Changes in REE fractionation induced by the halophyte plant *Halimione portucaloides,* from SW European salt marshes. Mar. Chem. 223, 103805.
Cao, Y., Shao, P., Chen, Y., Zhou, X., Yang, L., Shi, H., Yu, K., Luo, X., Luo, X., 2021. A critical review of the recovery of rare earth elements from wastewater by algae for resources recycling technologies. Resour. Conserv. Recycl. 169, 105519.
Costa, M., Henriques, B., Pinto, J., Fabre, E., Dias, M., Soares, J., Carvalho, L., Vale, C., Pinheiro-Torres, J., Pereira, E., 2020. Influence of toxic elements on the simultaneous uptake of rare earth elements from contaminated waters by estuarine macroalgae. Chemosphere 252, 126562.
Cunha, M.E. (2001). Physical Control of Biological Processes in a coastal upwelling system: comparison of the effects of coastal topography, river run-off and physical oceanography in the northern and southern parts of western Portuguese coastal waters. Dissertacão apresentada a Faculdade de Ciências da Universidade de Lisboa para obtencão do grau de doutor em Biologia, 305.
Davis, T.A., Volesky, B., Mucci, A., 2003. A review of the biochemistry of heavy metal biosorption by brown algae. Water Res. 37 (18), 4311–4330.
Elderfield, H., Upstill-Goddard, R., Sholkovitz, E.R., 1990. The rare earth elements in rivers, estuaries, and coastal seas and their significance to the composition of ocean waters. Geochim. Cosmochim. Acta 54, 971–991.
Feng, Z., Zhang, T., Shi, H., Gao, K., Huang, W., Xu, J., Wang, J., Wang, R., Li, J., Gao, G., 2020. Microplastics in bloom-forming macroalgae: distribution, characteristics and impacts. J. Hazard. Mater. 397, 122752.
Feng, Z., Zhang, T., Wang, J., Huang, W., Wang, R., Xu, J., Fu, G., Gao, G., 2021. Spatio-temporal features of microplastics pollution in macroalgae growing in an important mariculture area, China. Sci. Total Environ. 719, 137490.
Ferreira, N., Ferreira, A., Viana, T., Lopes, C.B., Costa, M., Pinto, J., Soares, J., Pinheiro-Torres, J., Henriques, B., Pereira, E., 2020. Assessment of marine macroalgae potential for gadolinium removal from contaminated aquatic systems. Sci. Total Environ. 749, 141488.
Figueiredo, C., Grilo, T.F., Lopes, C., Brito, P., Diniz, M., Caetano, M., Rosa, R., Raimundo, J., 2018. Accumulation, elimination and neuro-oxidative damage under lanthanum exposure in glass eels (*Anguilla anguilla*). Chemosphere 206, 414–423.
Figueiredo, C., Raimundo, J., Lopes, A.R., Lopes, C., Rosa, N., Brito, P., Diniz, M., Caetano, M., Grilo, T.F., 2020. Warming enhances lanthanum accumulation and toxicity promoting cellular damage in glass eels (Anguilla anguilla). Environ. Res. 191, 110051.
Figueiredo, C., Grilo, T.F., Lopes, C., Brito, P., Caetano, M., Raimundo, J., 2022. Lanthanum and Gadolinium availability in aquatic mediums: new insights to ecotoxicology and environmental studies. J. Trace Elem. Med. Biol. 71, 126957.
Fletcher, R.L., 1996. The occurrence of 'green tides' a review. In: Schramm W, Nienhuis PH (eds) Marine benthic vegetation: recent changes and the effects of eutrophication. Springer, Berlin 7–43.
Gao, G., Zhong, Z., Zhou, X., Xu, J., 2016. Changes in morphological plasticity of Ulva prolifera under different environmental conditions: a laboratory experiment. Harmful Algae 59, 51–58.
Gao, G., Liu, Y., Li, X., Feng, Z., Wu, H., Xu, J., 2017. Expected CO2-induced ocean acidification modulates copper toxicity in the green tide alga *Ulva prolifera*. Environ. Exp. Bot. 135, 63–72.

Goecke, F., Jerez, C.G., Zachleder, V., Figueroa, F.L., Bišová, K., Řezanka, T., Vítová, M., 2015. Use of lanthanides to alleviate the effects of metal ion-deficiency in Desmodesmus quadricauda (Sphaeropleales, Chlorophyta). Front. Microbiol. 6, 2.
González, V., Vignati, D.A., Pons, M.N., Montarges-Pelletier, E., Bojic, C., Giamberini, L., 2015. Lanthanide ecotoxicity: First attempt to measure environmental risk for aquatic organisms. Environ. Pollut. 199, 139–147.
Gwenzi, W., Mangori, L., Danha, C., Chaukura, N., Dunjana, N., Sanganyado, E., 2018. Sources, behaviour, and environmental and human health risks of high-technology rare earth elements as emerging contaminants. Sci. Total Environ. 636, 299–313.
Habig, W.H., Pabst, M.J., Jakoby, W.B., 1974. Glutathione S-transferases: the first enzymatic step in mercapturic acid formation. J. Biol. Chem. 249 (22), 7130–7139.
Hatje, V., Bruland, K.W., Flegal, A.R., 2014. Determination of rare earth elements after pre-concentration using NOBIAS-chelate PA-1®resin: Method development and application in the San Francisco Bay plume. Mar. Chem. 160, 34–41.
Haxel, G., 2002. Rare earth elements: critical resources for high technology. Rare earth elements: critical resources for high technology, , 2nd87. US Department of the Interior, US Geological Survey.
Herrmann, H., Nolde, J., Berger, S., Heise, S., 2016. Aquatic ecotoxicity of lanthanum–a review and an attempt to derive water and sediment quality criteria. Ecotoxicol. Environ. Saf. 124, 213–238.
Hu, B., He, M., Jakubowski, N., Meinhardt, J., Meyer, F.M., Niederstraßer, J., Schramm, R., Sindern, S., Stosch, H.G., Bertau, M., 2017. Handbook of Rare Earth Elements: Analytics. Walter de Gruyter GmbH & Co KG.
IPCC, 2021: Summary for policymakers. In: Climate Change 2021: The Physical Science Basis. Contribution of Working Group I to the Sixth Assessment Report of the Intergovernmental Panel on Climate Change [Masson-Delmotte, V., P. Zhai, A. Pirani, S.L. Connors, C. Péan, S. Berger, N. Caud, Y. Chen, L. Goldfarb, M.I. Gomis, M. Huang, K. Leitzell, E. Lonnoy, J.B.R. Matthews, T.K. Maycock, T. Waterfield, O. Yelekçi, R. Yu, and B. Zhou (eds.)]. In Press.
Ippolito, M., Fasciano, C., d'Aquino, L., Morgana, M., Tommasi, F., 2010. Responses of antioxidant systems after exposition to rare earths and their role in chilling stress in common duckweed (Lemna minor L.): a defensive weapon or a boomerang? Arch. Environ. Contam. Toxicol. 58 (1), 42–52.
Jacinto, J., Henriques, B., Duarte, A., Vale, C., Pereira, E., 2018. Removal and recovery of critical rare elements from contaminated waters by living Gracilaria gracilis. J. Hazard. Mater. 344, 531–538.
Johansson, L.H., Borg, L.H., 1988. A spectrophotometric method for determination of catalase activity in small tissue samples. Anal. Biochem. 174 (1), 331–336.
Joonas, E., Aruoja, V., Olli, K., Syvertsen-Wiig, G., Vija, H., Kahru, A., 2017. Potency of (doped) rare earth oxide particles and their constituent metals to inhibit algal growth and induce direct toxic effects. Sci. Total Environ. 593, 478–486.
Kirk, J., Allen, R., 1965. Dependence of chloroplast pigment synthesis on protein synthesis: effect of actidione. Biochem. Biophys. Res. Commun. 21 (6), 523–530.
Kovaříková, M., Tomášková, I., Soudek, P., 2019. Rare earth elements in plants. Biol. Plant. 63 (1), 20–32.
Lowry, O.H., Rosebrough, N.J., Farr, A.L., Randall, R.J., 1951. Protein measurement with the Folin phenol reagent. J. Biol. Chem. 193, 265–275.
Maulvault, A.L., Custódio, A., Anacleto, P., Repolho, T., Pousão, P., Nunes, M.L., Diniz, M., Rosa, R., Marques, A., 2016. Bioaccumulation and elimination of mercury in juvenile seabass (Dicentrarchus labrax) in a warmer environment. Environ. Res. 149, 77–85.
Migaszewski, Z.M., Gałuszka, A., 2015. The characteristics, occurrence, and geochemical behavior of rare earth elements in the environment: a review. Crit. Rev. Environ. Sci. Technol. 45 (5), 429–471.
Ngwenya, B.T., Mosselmans, J.F.W., Magennis, M., Atkinson, K.D., Tourney, J., Olive, V., Ellam, R.M., 2009. Macroscopic and spectroscopic analysis of lanthanide adsorption to bacterial cells. Geochim. Cosmochim. Acta 73 (11), 3134–3147.
Olivares, H.G., Lagos, N.M., Gutierrez, C.J., Kittelsen, R.C., Valenzuela, G.L., Lillo, M.E. H., 2016. Assessment oxidative stress biomarkers and metal bioaccumulation in macroalgae from coastal areas with mining activities in Chile. Environ. Monit. Assess. 188 (1), 1–11.
Pereira, P., de Pablo, H., Rosa-Santos, F., Pacheco, M., Vale, C., 2009. Metal accumulation and oxidative stress in Ulva sp. substantiated by response integration into a general stress index. Aquat. Toxicol. 91 (4), 336–345.
Pinto, J., Costa, M., Henriques, B., Soares, J., Dias, M., Viana, T., Ferreira, N., Vale, C., Pinheiro-Torres, J., Pereira, E., 2021. Competition among rare earth elements on sorption onto six seaweeds. J. Rare Earths 39 (6), 734–741.
Pinto, J., Henriques, B., Soares, J., Costa, M., Dias, M., Fabre, E., Lopes, C.B., Vale, C., Pinheiro-Torres, J., Pereira, E., 2020. A green method based on living macroalgae for the removal of rare-earth elements from contaminated waters. J. Environ. Manag. 263, 110376.
Rodrigues, L.A., Cardeira, M., Leonardo, I.C., Gaspar, F.B., Redovniković, I.R., Duarte, A. R.C., Paiva, A., Matias, A.A., 2021. Deep eutectic systems from betaine and polyols–Physicochemical and toxicological properties. J. Mol. Liq. 335, 116201.
Rogowska, J., Olkowska, E., Ratajczyk, W., Wolska, L., 2018. Gadolinium as a new emerging contaminant of aquatic environments. Environ. Toxicol. Chem. 37, 1523–1534.
Smith, V.H., Tilman, G.D., Nekola, J.C., 1999. Eutrophication: impacts of excess nutrient inputs on freshwater, marine, and terrestrial ecosystems. Environ. Pollut. 100 (1-3), 179–196.
Sun, Y., Oberley, L.W., Li, Y., 1988. A simple method for clinical assay of superoxide dismutase. Clin. Chem. 34 (3), 497–500.
Trapasso, G., Chiesa, S., Freitas, R., Pereira, E., 2021. What do we know about the ecotoxicological implications of the rare earth element gadolinium in aquatic ecosystems? Sci. Total Environ. 781, 146273.
Tyler, G., 2004. Rare earth elements in soil and plant systems-a review. Plant Soil 267 (1), 191–206.
Uchida, N., Matsukami, H., Someya, M., Tue, N.M., Viet, P.H., Takahashi, S., Tanabe, S., Suzuki, G., 2018. Hazardous metals emissions from e-waste-processing sites in a village in northern Vietnam. Emerg. Contam. 4 (1), 11–21.
Uchimura, M., Yoshida, G., Hiraoka, M., Komatsu, T., Arai, S., Terawaki, T., 2004. Ecological studies of green tide, *Ulva* spp.(chlorophyta) in hiroshima bay, the seto inland sea. Jpn. J. Phycol. 52, 17–22.
Uchiyama, M., Mihara, M., 1978. Determination of malonaldehyde precursor in tissues by thiobarbituric acid test. Anal. Biochem. 86 (1), 271–278.